Chapter

Evaluation by Monte Carlo Simulation of Doses Distribution in Tumors with Hypoxia

Mirko Salomón Alva-Sánchez and Thatiane Alves Pianoschi

Abstract

Radiotherapy is one of the most useful modalities applied for tumor treatments, which use ionization radiation to eradicate the tumor, in major cases. Cells with normal oxygenation are more sensitive to the effects of ionizing radiation than those with hypoxic conditions, because O_2 molecules react rapidly with free radicals, produced by irradiation, originating highly reactive radicals. Thus, the different concentrations of hypoxia in tumors can modulate the response of the irradiation through the radioresistance they present and consequently the success of the treatment. This chapter deals with the dose distributions in cranial tumors with different concentrations of hypoxia through a code based on Monte Carlo simulation.

Keywords: radiotherapy, tumor hypoxia, dose distribution, Monte Carlo simulations

1. Introduction

The modality of treatment with ionization radiation, specifically, for cancer can be considered routinely in several hospital centers, which must have human and technological resources capable of conforming the radiation dose into the target volumes and trying to avoid high toxicity in the adjuvant tissues. Although all these resources exist, the treatment planning is based on prior knowledge of the structures of the patient that can be obtained through any kind of medical images. Once the tumor has been diagnosed, appropriate treatment is indicated without, often, considering some factors that may influence treatment success, due the limitation of the medical images. Factors known as repair of sublethal DNA damage, cell repopulation, redistribution of cells, and reoxygenation are not considered [1].

Experimental data showed that oxygen is the most component that modified the radiation sensitivity and hypoxic cells that can be 2–3 times more resistant to ionizing radiation, which would imply administering doses higher than doses to achieve the same effect in oxygenated cells under normal conditions [2–4].

An important concept in clinical radiobiology is that the tumor may have subpopulations in hypoxic areas, thus leading to success of radiotherapy. Still, there are concepts related to acute or chronic hypoxic cells that may also alter treatment outcomes [5]. The low concentration of oxygen or hypoxia in the tumor tissues is a radiobiological phenomenon that has been observed since the beginning of the twentieth century [6].

The dependence of oxygen in tissue is related with the generation of free radicals, which came from interacting between the radiation energy and tissues. The quantity that measures the likelihood of this interacting is the cross section, which decreases when the beam energy increases [7]. Thus, few radicals will interact with the DNA of the tumor cell and consequently decreasing the chain reaction. This dependence is known as the oxygen effect that is ignored in the accuracy of ionization radiation treatments [8, 9], which is why hypoxia characterizes a tissue as radioresistant. Therefore, hypoxia and radiosensitivity are related to lower oxygen concentration rate; there will be higher survival cell rate, in postirradiation. On the other hand, there is an optimal oxygenation value wherewith the radiosensitivity increases [10]. Concentrations of oxygen in some tumors can be found in different regions in the same tumor complex. In this case, the tumor hypoxia may occur in a chronic or acute form. A form of oxygen concentration is due to the accelerated growth of the tumor in the most central parts, which are usually originated by the lack of adequate blood supply. In this way, in an axial section of one tumor, have concentric circles of regions of different oxygenation, whose central areas are necrotic [4]. One way to express the decreased radiosensibilty of cell, due to hypoxia, is through the parameter oxygen enhancement ratio (OER), which is defined as the amount of dose reduction required for cell of a given oxygenation level compared to cell with no oxygen to obtain the same effect [11].

One way to study the oxygen effect in tumors is through computational modeling. Thus, different modeling of oxygen effect has been proposed such as a voxel-based multiscale tumor response model [12]. The model used in this work was written in C++ simulating a virtual tumor with considering biological parameters as vascular fraction that is related to the oxygenation of the tumor.

Laura Antonovic and co-authors [13] used a treatment planning system TRiP [14] to simulated spherical tumors in silico based on a biological model of oxygen diffusion [15]. The beam used was carbon ion.

Another publication showed the use of a computational model for trans-vascular oxygen transport and blood vessel networks in tumors [16, 17].

The paper title *Dose prescription and optimisation based on tumor hypoxia* [18] proposed a method to prescribe dose distributions in radioresistant tumors.

The Monte Carlo HYP-RT model was used to simulate tumors considering the repopulation and reoxygenation for hypoxic head and neck tumors [19].

A 4D cellular model was applied to simulate head and neck cancer with oxygenation varying with vascularity and blood oxygenation [20].

An algorithm implemented on Geant4-DNA (codes based on Monte Carlo) was developed to show the effect of oxygen on DNA [21].

The Monte Carlo simulation, specifically the codes based on this method, can also be an effective dosimetric tool for the study of dose deposited. The dose–response from the codes shows an advantage of providing detailed studies in different conditions that involve procedures which are lengthy, complex, and expensive. The most commonly used Monte Carlo simulation codes in radiotherapy simulations are EGS, MCNP, and PENELOPE [22–28]. The quality of the results provided by the different codes is directly related to the accuracy of the implemented transport model and its data libraries associated with the cross section of the transported particles. Thus, the mixed charged particle transport algorithm, implemented by the penetration and energy loss of positron and electrons (PENELOPE) code [29], led to its intense use in radiotherapy [30–35].

This chapter presents a study of dose distribution in simulated cranial tumor with different concentrations of oxygen [18, 36–39] through the PENELOPE simulation code, which is based on the Monte Carlo method [40, 41]. The tumor with different concentrations of oxygen will be compared with one under normal oxygen conditions.

1.1 PENELOPE-Monte Carlo code

PENELOPE is a code used to simulate the transport of electrons, positrons, and photons considering interactions of photons and charged particles (such as the photoelectric effect, Rayleigh scattering, Compton scattering, production and annihilation of pairs, elastic and inelastic collisions), which are simulated in complex geometries and arbitrary materials.

In the PENELOPE package, there are subroutines written in FORTRAN distributed in various (open) source codes, applications, a database with characteristics of various materials, as well as application examples. The FORTRAN subroutines are organized into four basic files: PENELOPE.f, PENGEOM.f, PENVARED.f, and TIMER.f.

PENELOPE.f contains the simulated particle scattering and absorption subroutines, primary and secondary particle generation and storage, and particle transport management and simulation as a whole.

PENGEOM.f defines the structures, or geometries, to be simulated, which may consist of several homogeneous bodies, defined by a specified material and also by their limits in space. The bounding surfaces of the geometry bodies are described by quadratic functions. Through these functions surfaces such as planes, plane pairs, spheres, cylinders, cones, ellipsoids, parables, and hyperboloids can be defined.

For each body defined in the geometry file of a given simulation, a material index must be defined, corresponding to the material that will be a constituent of the body, having an agreement between the geometry file and the material file. In the material archive, the interaction data of the radiation with the material being used are shown in tables, as interaction coefficients for electrons and photons in energies from 1 eV to 1GeV. A material file is created using the subroutines of the MATERIAL.f and PENELOPE.f source codes. One of the advantages of PENELOPE is that it uses a recent database with the characteristics of various materials of interest in radiological physics [42] and current cross section libraries and other quantities required for particle transport [43].

The PENVARED.f source code contains subroutines that perform the variational reduction methods of the code, without increasing simulation time and neither the statistical uncertainty of the simulated results.

Finally, source code TIMER.f manages the simulation time.

The simulation algorithm is based on a model that combines numerical and analytical cross section data for the different types of interaction and is applied for initial energies from 1 keV to 1 GeV. Photons transport are simulated by the conventional or detailed, and for electron and positron are simulated using a mixed algorithm. Thus, for electrons and positrons, the PENELOPE code differs from other simulation codes by using a mixed algorithm that implements two simulation models: the detailed, for strong events, defined from angular deflection (scattering angle) or energy loss above a set value, and the condensate for weak interactions with angular deflection or energy loss less than the preset values. Condensed interactions are described by a multiple-scatter approximation consisting of transforming a given number of weak interactions into a single artificial event [44]. To develop a simulation with PENELOPE, the user must edit a FORTRAN file, user.f, with calls from the subroutines PENELOPE.f, PENGEOM.f, PENVARED.fe, and TIMER.f, providing overall simulation management and creating with these five FORTRAN files a user.exe file.

The simulation is started by running the user.exe file that reaches the user-supplied input information through the input.in file, geometry information through the geometry.geo file, and cross section information for the materials involved in the simulation through the material.mat file.

Another executable program comes together with PENELOPE package, the GEOVIEW.exe, which allows the visualization of the defined bodies and the materials that constitute a simulation geometry.

1.2 Simulation of the dose distribution in tumors with hypoxia through PENELOPE code

As some tumors have concentric circles of regions of low concentration of oxygenation, which are deprived of adequate blood supply, the evaluation of those regions becomes essential to guarantee the success of radiotherapy treatments [4]. The study evaluated the hypoxia effect in the dose distribution for simulated cranial tumor with different concentrations of oxygen [18, 36–39] through the PENELOPE simulation code. The code allows the "construction" of tumors through the compound's chemical composition, mass density, mean excitation energy, and energy and oscillator strength [45, 46]. The tumor with different concentrations of oxygen will be compared with one under normal oxygen conditions. The parameter OER was applied to express the decreased radiosensibilty of the tumor with hypoxia. The simulation of the dose distribution in tumors with hypoxia through PENELOPE code is based on the published by Alva-Sánchez [47].

2. Material and methods

The Monte Carlo code, PENELOPE®, version 2008 was used to achieve the main objective to simulate tumors with hypoxia. Since the code allows the "construction" of materials by the compound's chemical composition, the soft tissue material from the code, number 262, was modified by adding different concentrations tumors with hypoxia, from knowledge that chemical compounds of the normal tissue are approximately equal to the tumor. The geometry of simulation used was a parallelepiped of $8 \times 15 \times 21$ cm^3 containing six identical spherical tumors of 1.2 cm radius, as shown in **Figure 1** [47]. In that work 2×10^9 primary particles and 0.1mm^2 pixel size and photon spectra at 6 MV [48], which was applied in the input file of the code, were used. The tumors were located before the buildup region for the

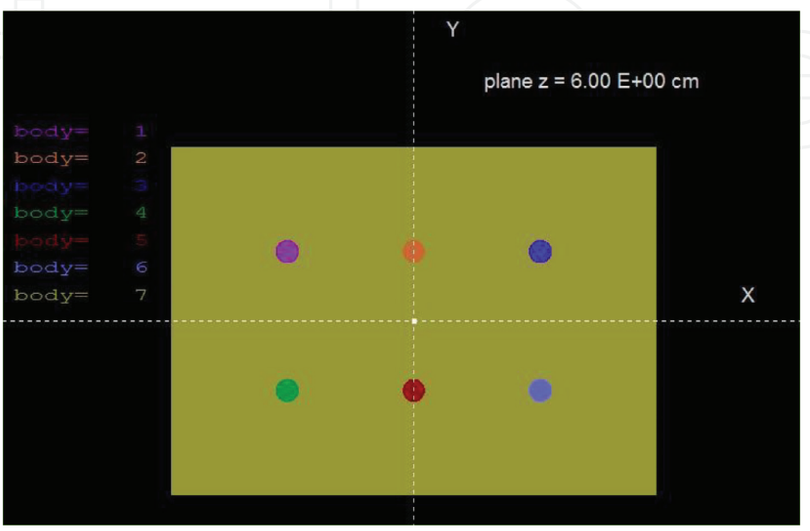

Figure 1.
Geometric representation through of the PENELOPE code, for the simulation of six tumors (spheres) spaced within the parallelepiped, in the XY plane.

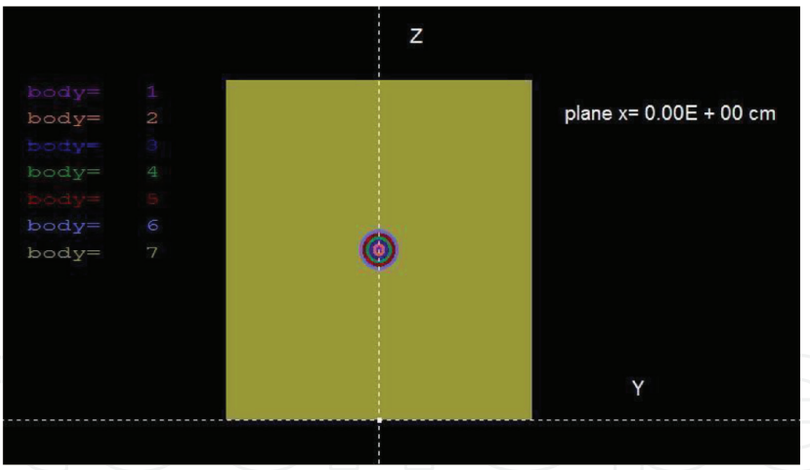

Figure 2.
Geometric representation of the PENELOPE code, for the simulation of a tumor (sphere) centralized in the center of the brain (cylinder), in the ZY plane.

6 MV beam at 10 cm from the top of the phantom. The simulated material of the parallelepiped was a soft tissue, available in the code, while the tumors had different pressures of oxygen, from 5 to 70 mmHg. Simulation responses were obtained through the values average in the whole target or spherical tumors.

This geometry used to simulate the radiation conditions was 22 × 22 cm^2 radiation field, 100 cm source-tumor distance, with a 6 MV energy beam. The obtained results from the simulation were analyzed in terms of deposited energy and values of OER relative to the pressure O_2 in terms of mmHg, following the OER equation proposed for [55].

$$OER = 1 + 0.81\left(pO_2{}^{0.616}\right)/\left(1 + pO_2{}^{0.616}\right) \quad (1)$$

The second part of that work published [47] analyzed the oxygen effect in the dose distributions in simulated cranial tumors: one with different oxygen concentrations and the other with normal oxygenation [18, 36–39]. A cylinder with 18 cm in diameter and 20 cm in height was simulated to represent the head of an adult, containing concentric spheres of radii of 0.5–1.2 cm that can represent the dimensions of a glioblastoma tumor. Due the characteristics of localization of this kind of tumor, the simulation tumors were centralized at 10 cm height, beyond the equilibrium range to charged particle for the energy used in this study. The bean incident was simulated in the direction to the phantom, parallel to the Z axis. In **Figure 2** the geometry for radiation for a simulated tumor with different concentrations of oxygen from minor (radius sphere 0.5 cm) to greater is shown (radius sphere 1.2 cm).

The simulated material of the tumors and brain structures was soft tissue due to similar chemical compounds present. This material is available in the simulation code. In the spheres (tumors) these materials were modified with different concentrations of oxygen. The radiation conditions used were 1.2 × 1.2 cm radiation field, source-tumor distance of 100 cm, and photon spectra at 6 MV.

3. Results

From the results obtained to the six spheres inserted in the parallelepiped (**Figure 1**), the deposited energy was plotted for each spherical tumor containing

different pressures of oxygen as shown in **Figure 3**. Values of the OER were obtained through Eq. (1) and plotted for each pressure of oxygen, as shown in **Figure 4**.

The *penmain* file of the code generates an output file with generic information, such as number of simulated primary showers, secondary-particle generation probabilities, average deposited energies, and statistical error, etc. Each simulation was written in a separate file. The program computes and delivers the statistical uncertainties (3σ) of all evaluated quantities and distributions. Thus, for all obtained results, an error at least 3.58% was reported by the code used.

Figure 5a shows the dose distributions for a simulated tumor of 1.2 cm radius with different pressures of O_2, and **Figure 5b** shows the same tumor of **Figure 5a** with normal oxygenation.

These distributions were compared through a dose profile, as shown in **Figure 6**, along the center of the dose maps.

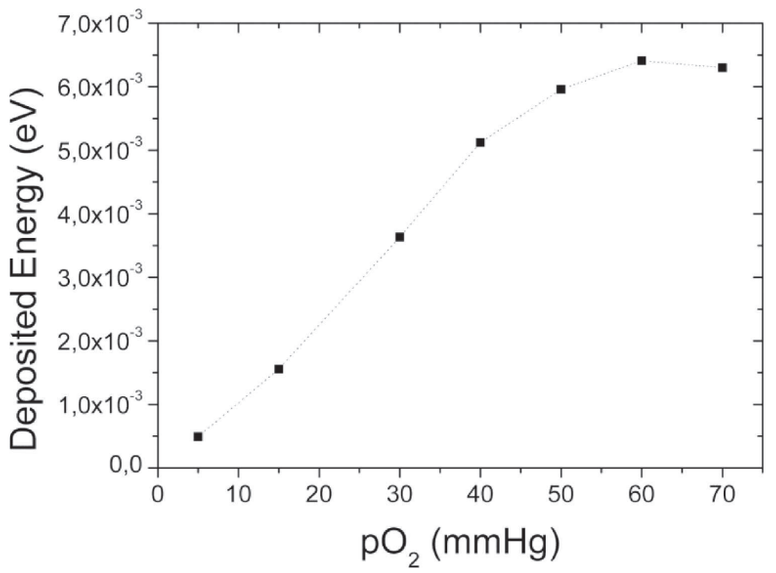

Figure 3.
Behavior and deposited energy for six identical spheres with different pressures of O_2.

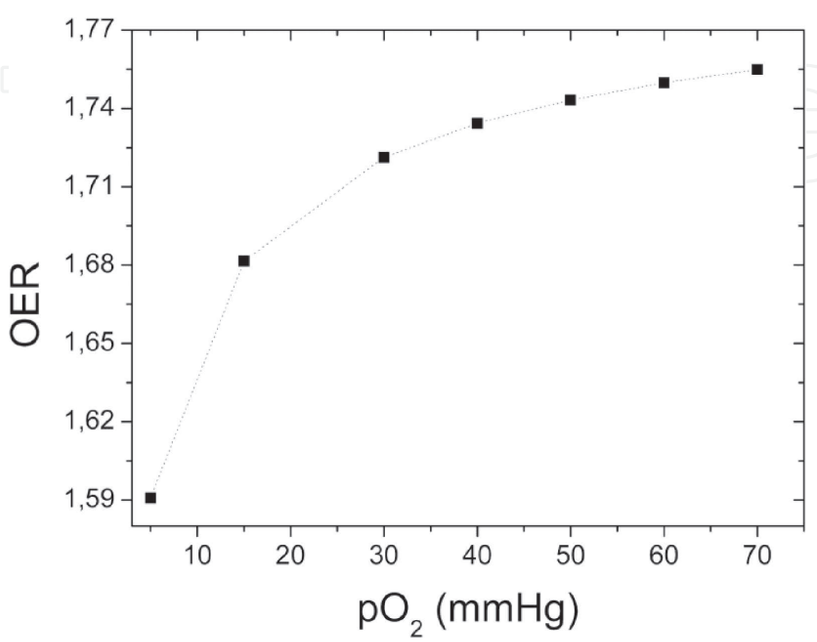

Figure 4.
OER values relative to each of the six identical spheres with different pressures of O_2.

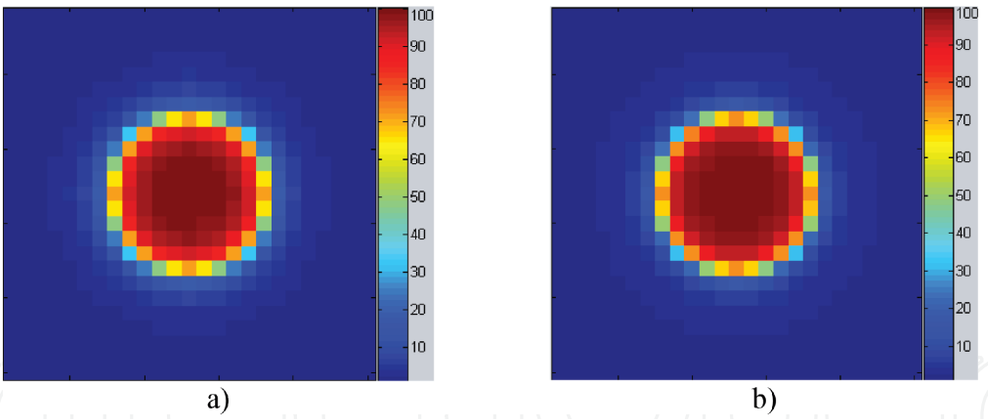

Figure 5.
Dose distribution of the tumor of 7.24 cm³: (a) tumor 1, with different pressures O_2, and (b) tumor 2, normal oxygenation.

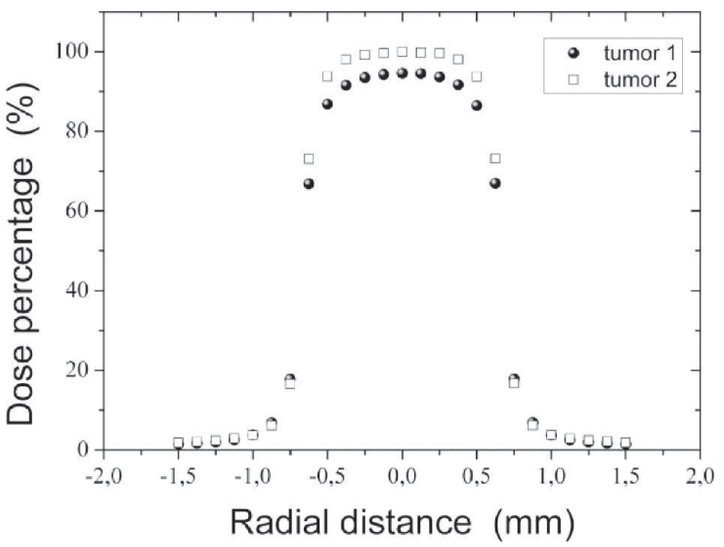

Figure 6.
Dose relative profile of tumor 1 (with different pressures of O_2) and tumor 2 (with normal oxygenation).

4. Discussions and conclusions

Statistical uncertainties at least 3.58% was reported by the code for all simulations. From the results shown in **Figure 3**, we can observe that the deposited energy have an approximately linear behavior with the increases in pressure until 50 mmHg of O_2; from this pressure the deposited energy shows a constant trend for higher pressures than 60 mmHg of O_2. This behavior was also equivalent to those presented in the literature [36, 49].

The obtained values of the OER relative to pressure of O_2 shown in **Figure 4** have a behavior similar to an increasing logarithm function as found in literature [50–54]. After the 60 mmHg of pressure of O_2, the OER values have a trend to value constant. **Figures 3** and **4** confirm the increasing of the deposited energy for tumors with a high concentration of oxygen, because of the oxygen effect that is disregarded in accuracy of the ionization radiation treatment [53, 55].

The dose distributions shown in **Figure 5** visually show almost the same distribution, but in the field profile of both distributions, shown in **Figure 6**, a difference of 7.29% was found at a radial distance of 0.6 mm of the tumor. The code allowed evaluated the influences of effect of oxygen for tumors with hypoxia that is related

with the outcome of treatment with radiotherapy. However, the hypoxic tumor cells are resistant to radiation [8]. From the comparisons of the dose distribution in the central plane of the phantom, it was observed that there are regions where the concentration of oxygen was lower (that of sphere of less radius), thus, the energy deposited was lower, unlike the spheres with higher oxygen concentrations.

Despite the fact that the code cannot simulate the physiological factor, which it can modulate a variety of normal developmental and metabolic processes that cause injury to the tumor cell, the present study of tumors with hypoxia plays an important role in dose distribution that can compromise the treatment outcomes and individual prognosis.

5. Considerations

There are a number of simulation and numerical methods and codes that demonstrate the importance of the low concentration oxygen effect in response to ionizing radiation treatments. This chapter shows the work *Study of the distribution of doses in tumors with hypoxia through the PENELOPE code* which showed physical parameters with results similar to the literature through the PENELOPE-Monte Carlo code.

Acknowledgements

The authors thank professor Ph.D. Patricia Nicolucci for her orientation and suggestions for all the works, which are part of our doctorate work.

Author details

Mirko Salomón Alva-Sánchez* and Thatiane Alves Pianoschi
Department of Exact Science and Applied Social, Federal University of Health Sciences of Porto Alegre, Porto Alegre, Rio Grande do Sul, Brazil

*Address all correspondence to: mirko@ufcspa.edu.br

References

[1] Lind BK, Brahme A. The radiation response of heterogeneous tumors. Physica Medica. 2007;**23**:919

[2] Schwarz G. Ueber Desensibilisierung gegen Roentgen und Radium Strahlen. Muenchner Medizinische Wochenschrift. 1909;**24**:1-2

[3] Thomlinson RH, Gray LH. The histological structure of some human lung cancers and the possible implications for radiotherapy. British Journal of Cancer. 1955;**9**:539-549

[4] Hall EJ, Giaccia AJ. Radiobiology for the Radiologist. 6th ed. Philadelphia: Lippincott Williams & Wilkins; 2006

[5] Bristow RG, Hill RP. Hypoxia and metabolism. Hypoxia, DNA repair and genetic instability. Nature Reviews. Cancer. 2008;**8**(3):180-192

[6] De olveira R, Alves R. Agentes antineoplásicos biorredutiveis: uma nova alternativa para o tratamento de tumores sólidos. Quimica Nova. 2002;**25**(6):976-984

[7] Itikawa Y. Cross sections for electron collisions with oxygen molecules. The Journal of Physical Chemistry. 2009;**38**:1

[8] Wenzl and Wilkins. Theoretical analysis of the dose dependence of the oxygen enhancement ratio and its relevance for clinical applications. Radiation Oncology. 2011;**6**:171

[9] Yamashitaa S, Katsumurab Y, Linc M, Muroyad Y, Miyazakia T, Murakamie T. Water radiolysis with heavy ions of energies up to 28 GeV. 1. Measurements of primary g values as track segment yields. Radiation Physics and Chemistry. 2008;**77**:439-446

[10] Nias A. An Introduction to Radiobiology. 2nd ed. Chichester: Wiley; 2000

[11] Anon. Quantitative Concepts and Dosimetry in Radiobiology. International Commission on Radiation Units and Measurements. ICRU Report 30. Bathesda, MD; 1979

[12] Espinoza I, Peschke P, Karger CP. A voxel-based multiscale model to simulate the radiation response of hypoxic tumors. Medical Physics. 2015;**42**:90-102. DOI: 10.1118/1.4903298

[13] Antonovic L, Lindblom E, Daşu A, Bassler N, Furusawa Y, Toma-DAşu I. Clinical oxygen enhancement ratio of tumors in carbon ion radiotherapy: The influence of local oxygenation changes. Journal of Radiation Research. 2014;**55**:902-911

[14] Krämer M, Scholz M. Treatment planning for heavy-ion radiotherapy: Calculation and optimization of biologically effective dose. Physics in Medicine and Biology. 2000;**45**:3319-3330

[15] Daşu A, Toma-Daşu I, Karlsson M. Theoretical simulation of tumour oxygenation and results from acute and chronic hypoxia. Physics in Medicine & Biology. 2003;**48**:2829-2842

[16] Welter M, Fredrich T, Rinneberg H, Rieger H. Computational model for tumor oxygenation applied to clinical data on breast tumor hemoglobin concentrations suggests vascular dilatation and compression. PLoS One. 2016;**11**(8):e0161267. DOI: 10.1371/journal.pone.0161267

[17] Gödde R, Kurz H. Structural and biophysical simulation of angiogenesis and vascular remodeling. Developmental Dynamics. 2001;**220**(4):387-401

[18] Toma-Daşu I, Daşu A, Brahme A. Dose prescription and optimisation based on tumour hypoxia. Acta Oncologica;**48**:2009, 11811192

[19] Harriss-Phillips WM, Bezak E, Yeoh EK. Monte Carlo radiotherapy simulations of accelerated repopulation and reoxygenation for hypoxic head and neck cancer. The British Journal of Radiology. 2011;**84**(1006):903-918. DOI: 10.1259/bjr/25012212

[20] Forster JC, MJJ D, Harriss-Phillips WM, Bezak E. Simulation of head and neck cancer oxygenation and doubling time in a 4D cellular model with angiogenesis. Scientific Reports. 2017;**7**(1):11037. DOI: 10.1038/s41598-017-11444-1

[21] Forster JC, MJJ D, Phillips WM, Bezak E. Monte Carlo simulation of the oxygen effect in dna damage induction by ionizing radiation. Radiation Research;**190**(3):248-261

[22] De Vlamynck K et al. Dose measurements compared with Monte Carlo simulations of narrow 6 MV multifead collimator shaped photon beams. Medical Physics. 1999;**26**:1874-1882

[23] Pooter JA et al. Computer optimization of nocoplanar beam setups improves stereotactic treatment of liver tumors. International Journal of Radiation Oncology Biology Physics. 2006;**66**:913-922

[24] Yamamoto T et al. An integrated Monte Carlo dosimetric verification system for radiotherapy treatment planning. Physics in Medicine and Biology. 2008;**52**:1991

[25] Ghassoun J, Senhou N, Jehouani A. Neutron and photon doses in high energy radiotherapy facilities and evaluation of shielding performance by Monte Carlo method. Annals of Nuclear Energy. 2011;**38**(10):2163-2167

[26] Kim JH, Hill R, Kuncic Z. An evaluation of calculation parameters in the EGSnrc/BEAMnrc Monte Carlo codes and their effect on surface dose calculation. Physics in Medicine and Biology. 2012;**57**(4):N267-N278

[27] Rodriguez M, Sempau J, Brualla L. Combined approach of variance reduction techniques for the efficient Monte Carlo simulation of linacs. Physics in Medicine & Biology. 2012;**57**(10)

[28] Martinez-Rovira I, Sempau J, Prezado Y. Monte Carlo-based treatment planning system calculation engine for microbeam radiation therapy. Medical Physics. 2012;**39**(5):2829-2838

[29] Sempau J et al. A PENELOPE-based system for the automated Monte Carlo simulation of clinacs and a voxelized geometries—Application to far-from-axis fields. Medical Physics. 2011;**38**(11):5887-5895

[30] Koivunoro H et al. Accuracy of the electron transport in MCNP5 and its suitability for ionization chamber response simulations: A comparison with the EGSNRC and PENELOPE codes. Medical Physics. 2012;**39**(3):1335-1344

[31] Ramirez VJ et al. Dosimetry of small radiation field in inhomogeneous medium using alanine/EPR minidosimeters and PENELOPE Monte Carlo simulation. Radiation Measurements. 2011;**46**:941-944

[32] Carvajal MA et al. Monte Carlo simulation using the PENELOPE code with ant colony algorithm to study MOSFET detectors. Physics in Medicine and Biology. 2009;**54**:6263-6276

[33] Górka B et al. Optimization of a tissue-equivalent CVD-diamond dosimeter for radiotherapy using the Monte Carlo code PENELOPE. Nuclear Instruments and Methods in Physics Research Section A. 2008;**59**(3):578-587

[34] Badal A et al. Monte Carlo simulation of a realistic anatomical

phantom described by triangle meshes: Application to prostate brachytherapy imaging. Radiotherapy and Oncology. 2008;**86**:99-103

[35] Brualla L et al. Comparison between PENELOPE and electron Monte Carlo simulations of electron fields used in the treatment of conjunctival lymphoma. Physical Biology. 2009;**54**:5469-5481

[36] Tuckwell W, Bezak E, Yeoh E, Marcu L. Efficient Monte Carlo modelling of individual tumor cell propagation for hypoxic head and neck cáncer. Physics in Medicine and Biology. 2008;**53**:4489-4507

[37] Diabira S, Morandi X. Gliomagenesis and neural stem cells: Key role of hypoxia and concept of tumor "neo-niche". Medical Hypotheses. 2008;**70**:96-104

[38] Evans S, Judy K, Dunphy I. Comparative measurements of hypoxia in human brain tumor using needle electrodes and EF5 binding. Cancer Research. 2004;**64**:1886-1892

[39] Wang J, Klem J, Wyrick J. Detection of hypoxia in human brain tumor xenografts using a modified comment assay. Neoplasia. 2003;**4**:288-296

[40] Salvat F, Fernández-Varea J, Sempau J. PENELOPE-2008: A Code System for Monte Carlo Simulation of Electron and Photon Transport, Nuclear Energy Agency OECD/NEA, Issy-les-Moulineaux, France. 2008. Available from: http://www.nea.fr

[41] Sempau J, Acosta E, Baró J, et al. An algorithm for Monte Carlo simulation of coupled electron-photon transport. Nuclear Instruments and Methods in Physics Research Section B. 1997;**1997**(132):377-390

[42] International Commission on Radiation Units and Measurements. Tissue substitutes in radiation dosimetry and measurement. ICRU report 44. Bethesda: EUA; 1989

[43] Salvat F, Fernández-Varea JM, Sempau J. A Code System for Monte-Carlo Simulation of Electron and Photon Transport, September, France. 2005

[44] Sempau J, Andreo P. Configuration of the electron transport algorithm of PENELOPE to simulate íon chambers. Physics in Medicine & Biology. 2006;**51**:3533-3548

[45] Alva M, Pianoschi1 T, Marques T, Santanna M, Baffa O, Nicolucci P. Monte Carlo simulation of MAGIC-f gel for radiotherapy using PENELOPE. Journal of Physics: Conference Series. 2010;**250**(1)

[46] Sánchez A, Salomón M. Verificação 3D da distribuição da dose em radiocirurgia estereotáxica através de simulação Monte Carlo e dosimetria por ressonância magnética nuclear. 2012. Tese (Doutorado em Física Aplicada à Medicina e Biologia) - Faculdade de Filosofia, Ciências e Letras de Ribeirão Preto, Universidade de São Paulo, Ribeirão Preto. 2012. DOI: 10.11606/T.59.2012.tde-15052013-193530. Acesso em: 2020-03-31

[47] Alva-Sánchez MS, Pianoschi TA. Study of the distribution of doses in tumors with hypoxia through the PENELOPE code. Radiation Physics and Chemistry. 2019;**167**:108428

[48] Sheik-Bagheri D, Rogers DWO. Monte Carlo calculation of nine megavoltage photon beam spectra using the BEAM code. Medical Physics. 2002;**29**:391-402

[49] Grimes DR, Warren DR, Warren S. Hypoxia imaging and radiotherapy: Bridging the resolution gap. The British Journal of Radiology. 2017 Aug;**90**(1076):20160939. DOI: 10.1259/bjr.20160939. [Epub May 25, 2017]

[50] Kirkpatrick J, Cárdenas-Navia LI, Dewhirst MW. Predicting the effect of temporal variations in PO_2 on tumor radiosensitivity. International Journal of Radiation Oncology Biology Physics. 2004;**59**(3):822-833

[51] Taha E, Djouider F, Banoqitah E. Monte Carlo simulations for dose enhancement in cancer treatment using bismuth oxide nanoparticles implanted in brain soft tissue. Australasian Physical & Engineering Sciences in Medicine. 2018;**41**:363-370

[52] Grimes R, Partridge M. A mechanistic investigation of the oxygen fixation hypothesis and oxygen enhancement ratio. Biomedical Physics & Engineering Express. 2015, 2015;**1**:045209

[53] Grimes R, Fletcher A, Partridge M. Oxygen consumption dynamics in steady-state tumor models. Royal Society Open Science. 2014;**1**:140080

[54] Alper T, Howard-Flanders P. Role of oxygen in modifying the radiosensitivity of *E. coli* B. Nature. 1956;**178**:978-979

[55] Ye SJ. Monte Carlo based protocol for cell survival and tumour control probability in BNCT. Physics in Medicine & Biology. 1999;**44**:447-461